OPEN ACCESS

Atmospheric Sciences REPORT

Increasing seasonal disparity in water availability across the Northern Hemisphere

Fubo Zhao,[1] Wenbo Shi,[1] Yiping Wu,[1,*] and Shuguang Liu[2]

*Correspondence: rocky.ypwu@gmail.com

Received: April 7, 2025; Accepted: January 7, 2026; Published Online: January 15, 2026; https://doi.org/10.59717/j.xinn-geo.2026.100191

GRAPHICAL ABSTRACT

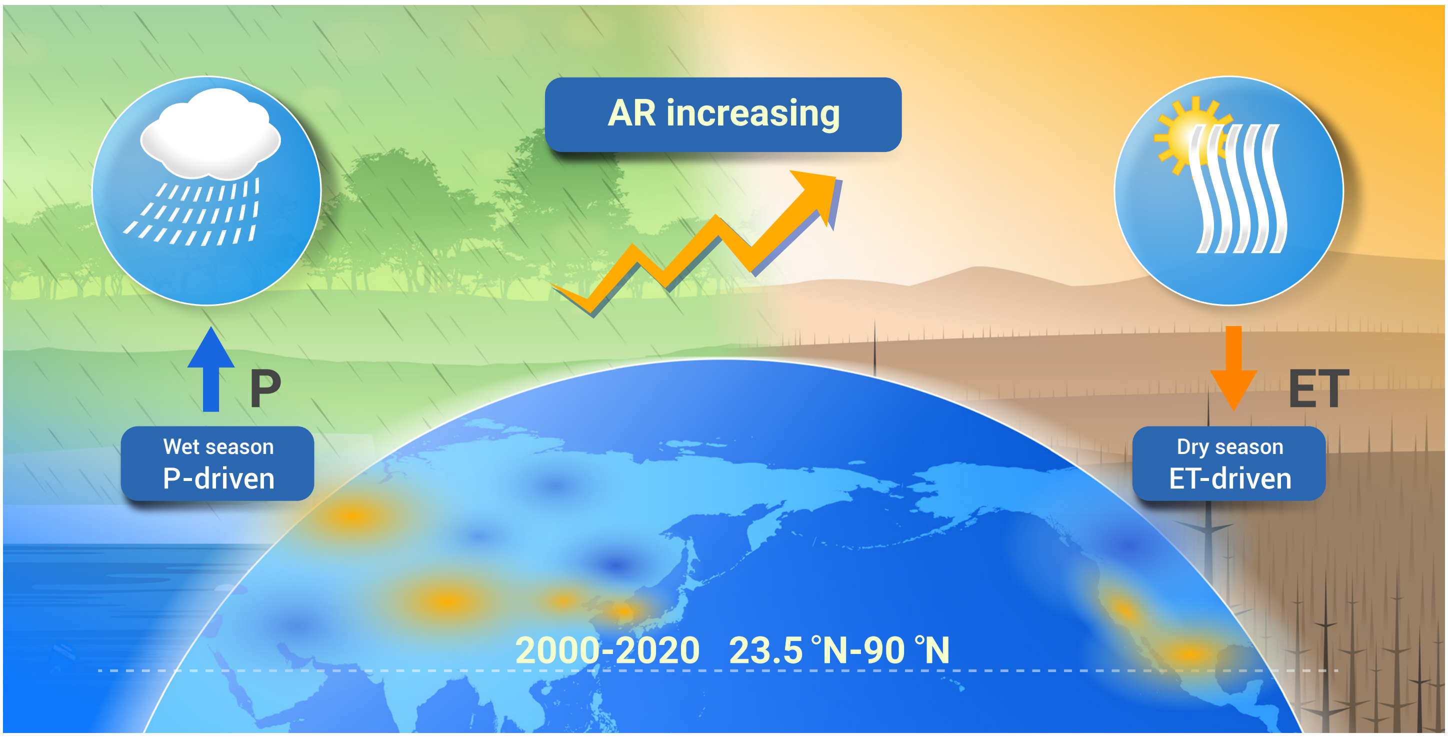

PUBLIC SUMMARY

- Seasonal disparity in land water availability have increased in recent decades.
- Wet season precipitation (P)–evapotranspiration (ET) rises and dry season P–ET falls due to P and ET changes.
- Most earth models can reproduce seasonal shifts in P–ET on a hemispheric scale.

Increasing seasonal disparity in water availability across the Northern Hemisphere

Fubo Zhao,[1] Wenbo Shi,[1] Yiping Wu,[1,*] and Shuguang Liu[2]

[1]Institute of Global Environmental Change, Department of Earth & Environmental Science, School of Human Settlements and Civil Engineering, Xi'an Jiaotong University, Xi'an 710049, China

[2]School of Ecology, Hainan University, Haikou 570228, China

*Correspondence: rocky.ypwu@gmail.com

Received: April 7, 2025; Accepted: January 7, 2026; Published Online: January 15, 2026; https://doi.org/10.59717/j.xinn-geo.2026.100191

Citation: Zhao F., Shi W., Wu Y., et al. (2026). Increasing seasonal disparity in water availability across the Northern Hemisphere. *The Innovation Geoscience* **4**:100191.

The water cycle, including the seasonal variations in land water availability (precipitation minus actual evapotranspiration (P–ET)), is intensifying with climate warming. These changes in P–ET, particularly the fluctuations between wet and dry seasons, have profound implications for ecosystem functioning and services. Understanding the dynamics and drivers of these changes is crucial for effective water resource management and climate adaptation strategies. Here, we examined seasonal P–ET changes based on multiple datasets across the extratropical Northern Hemisphere over the past two decades. Our results demonstrate a substantial increasing tendency in annual range between wet and dry season P–ET. Specifically, we observed that this trend is driven by both an increase in wet season P–ET and a decrease in dry season P–ET. Further analysis indicated that the changes in wet season P–ET were primarily due to changes in P, whereas the reductions in dry season P–ET were largely attributed to changes in ET. The results reveal a pronounced intra-hemispheric heterogeneity delineating P-dominated versus ET-dominated regimes. Evaluation of 32 state-of-the-art Earth System Models shows that most models capture these seasonal trends during recent decades, although some fail to do so. Our results highlight an enhanced seasonality in hemispheric water availability, driven by distinct changes in wet and dry season dynamics.

INTRODUCTION

Changes in water availability over land, which are denoted as precipitation (P) minus actual evapotranspiration (ET; P–ET), significantly influence livelihoods, socioeconomic development, and natural ecosystems.[1-5] With global warming, significantly accelerating moisture transport are anticipated, which will have profound impacts on P and ET and, thus, land water availability over land areas.[6-8] Particularly, the increased moisture cycle can also intensify the P–ET seasonal variations, which has shown clear evidence in ocean but remain complex over land.[9,10] The seasonal variations in P–ET, both in terms of space and time, has important implications for human lives, because it may be linked with floods and droughts and thus the water resources and ecosystem services.[11] Our previous work indicates a global intensification of P–ET seasonality; however, pronounced regional heterogeneity implies that similar emergent trends can arise from distinct underlying forces.[12] Therefore, it is crucial to identify regions where the seasonal patterns of P–ET have changed over land and determine the underlying driving forces.

The "wet get wetter, dry get drier" (WWDD) phenomenon is recognized as the consequence of seasonal alternations in P and ET occur across both space and time.[9,13-15] This phenomenon indicates that the wet regions/seasons getting wetter and dry regions/seasons getting drier. During the past few years, many studies have demonstrated that the seasonal WWDD concept has some applicability on a global scale.[13,14,16-18] However, at the regional scale, the validity of the WWDD paradigm is still uncertain.[19-21] For example, in some extratropical regions, there is evidence that the seasonal pattern of WWDD is valid.[17] In some dry regions, there was no evidence of the seasonal WWDD.[22] These differences can be attributed to disparities in the study periods (ranging from one to several decades), study scopes (spanning from regional to global scales), and datasets employed (model outputs and ground-based datasets) to estimate the land water availability.[1,23,24] Despite a recent study illustrating a declining trend in global water availability over the past twenty years (from 2001 to 2020),[2] there is still a lack of understanding of the alterations in the seasonal patterns of land water availability during this timeframe. Therefore, it is important to investigate the changes in seasonal water availability and its causal factors.

In this study, we assessed seasonal changes in P–ET choosing extratropical Northern Hemisphere (> 23.5° N) as the study area. We focused on the land water availability from 2000 to 2020 within the extratropical Northern Hemisphere regions because of its pivotal role in global socio-economic development.[4,25] We build on our recent global assessment of seasonal P–ET variability and apply the similar framework to the extratropical Northern Hemisphere to resolve regional mechanisms that are not depicted at global scale.[12] Specifically, we conducted the analysis using multiple remote sensing with ground-based precipitation and ET datasets, and quantified the dominant drivers using a simple attribution framework. The findings of this study could enhance our understanding of seasonal fluctuations in water availability at the regional scale.

MATERIALS AND METHODS

Precipitation and evapotranspiration datasets

We used three advanced diagnostic precipitation datasets from 2000 to 2020: the Climatic Research Unit gridded Time Series (CRU),[26] the Global Precipitation Climatology Center (GPCC),[27] and the Multi-Source Weighted-Ensemble Precipitation (MSWEP).[28] The CRU dataset provides monthly precipitation on a 0.5° grid over global land areas, derived from in situ station observations through interpolation. The GPCC offers gauge-based gridded precipitation analyses derived from quality-controlled rain-gauge station data, available at multiple spatial resolutions for land surfaces. The MSWEP dataset provides global three-hourly precipitation data at a 0.1° resolution, which were obtained from gauge, satellite, and reanalysis datasets.

We used three actual evapotranspiration products spanning 2000/2001-2020: the Global Land Evaporation Amsterdam Model (GLEAM),[29] the MODIS evapotranspiration product (MOD16A2),[30] and the Penman-Monteith-Leuning evapotranspiration product (PML-V2).[31] The GLEAM product provides monthly ET estimates at 0.25° spatial resolution for 2000-2020. The MODIS (MOD16A2) product offers 8-day ET data at 500 m resolution for 2001-2020. The PML-V2 product provides 8-day ET estimates at 500 m resolution over 2001-2020. All datasets were resampled to 0.5° using bilinear interpolation prior to estimating seasonal water availability to ensure spatial consistency across datasets. More detailed description of these data can be found in our previous study.[12]

Seasonal water availability estimation

The monthly water availability was calculated using P minus ET for each grid cell:[2,32,33]

$$[water\ availability]_{j,i} = P_{j,i} - ET_{j,i} \quad (1)$$

where j and i are the year and month, respectively. Since our study focused on seasonal water availability, we applied a three-month running average to the entire dataset to smooth short-term fluctuations as described in our previous study.[12] For each grid cell and each year, the wet season was defined as the three-month period corresponding to the maximum P–ET value, while the dry season was defined as the three-month period corresponding to the minimum P–ET value.[1,17] The difference between P–ET in the wet and dry seasons was then computed to quantify the amplitude of seasonal water availability variability. This approach ensured that the definitions of wet and dry seasons varied spatially and temporally, allowing them to adapt dynamically to interannual and regional hydrological variations. Furthermore, by identifying the wettest and driest periods based on P–ET extrema rather than fixed calendar months, this definition accounted for potential temporal shifts in seasonal patterns, thereby improving the accuracy of AR estimation in P–ET. To validate the seasonality and trend changes of P–ET, we collected runoff data from watersheds larger than 2,500 km^2 across the Northern Hemisphere, covering the study period from 2000 to 2020. Using the same methodology, we calculated the seasonal runoff trends and compared them with our estimations. The results showed that 61% of the watersheds were consistent with our predictions, while 31% of the discrepancies may be attributed to the omission of subsurface water storage changes.

Trends and the attribution analysis

We estimated trends in AR, wet season and dry season water availability at the grid scales using the non-parametric Mann-Kendall test, and quantified trend magnitudes using Sen's slope estimator.[34,35] The statistical significance was assessed based on the Mann-Kendall test results.[36,37] To isolate the respective contributions of P and ET to the trends in AR, we conducted simple factorial experiments using the approach described in our previous study.[12] In the real experiment, P–ET was calculated using the observed, time-varying P and ET. Two additional control experiments were performed by holding either P or ET fixed at its 2000 value while allowing the other variable to vary as observed, thereby separating their individual effects on the trends. The trend of the real-control difference was interpreted as the contribution of the fixed variable to the total change. For example, the contribution of P was quantified by recalculating monthly P–ET with P fixed at its 2000 value and ET varying as observed; the difference between this control run and the real experiment was attributed to P.

Earth system models

We analyzed outputs from 32 Coupled Model Intercomparison Project Phase 6 (CMIP6) Earth System Models (ESMs) to assess their ability to reproduce the seasonal patterns of water availability.[38,39] Model details are listed in Table S1.

RESULTS

Increasing range between the wet and dry season water availability

During the study period, the ensemble AR anomaly across the extratropical Northern Hemisphere increased significantly with a trend of 0.27 ± 0.05 mm yr^{-1} ($P < 0.01$; Figure 1A), which is higher than that of global trend.[12] To validate the seasonality and trend changes of P–ET, we collected runoff data from watersheds larger than 2,500 km^2 across the Northern Hemisphere, covering the study period from 2000 to 2020. Using the same methodology, we calculated the seasonal runoff trends and compared them with our estimations. The results showed that 61% of the watersheds were consistent with our predictions based on runoff alone. When incorporating GRACE ΔS, the agreement increased to 65%, highlighting the added value of GRACE ΔS in capturing seasonal water storage variations and providing a more robust validation of P–ET (Figure S1). This significant increasing trend in the AR anomaly was unique when compared with the other areas across globe using same datasets (Tropics trend = -0.18 mm yr^{-1} and Southern Hemisphere trend = -0.30 mm yr^{-1}), and there was also a slight increasing trend in the global AR anomaly (Figure S2). This increase in the AR aligns with prior research, which suggests that global warming elevates water vapor levels in the atmosphere and intensifies horizontal water vapor transport, thereby reinforcing the seasonal cycle of water availability.[1,14,15] This temporal increasing trend in the AR anomaly was also observed in the individual combinations (trends ranging from 0.20 mm yr^{-1} to 0.37 mm yr^{-1}; Figure S3). Over two-thirds of the land areas (68.1%) displayed increasing trends in the AR, which suggests a widespread shift in the regime (Figure 1B). Significant increasing trends ($P < 0.05$) were detected over 9.4% among these areas. By contrast, AR declined over 31.9% of the land surface, with significant decreases confined to 1.5% ($P < 0.05$). The change in the AR also displayed an obvious latitude pattern, with high increasing rates in the temperate region (23.5°–50° N) and relatively low increasing rates in the boreal regions (> 50°N; Figure 1C). This spatial trend in the AR was also confirmed by each individual investigation (Figure S4).

The spatiotemporal trends in the wet and dry season P–ET were examined (Figure 2). During 2000–2020, the wet season P–ET increased significantly, with a rate of 0.15 ± 0.05 mm yr^{-1} ($P < 0.01$; Figures 2A & S5-S6), but the dry season P–ET decreased significantly, with a decreasing rate of -0.12 ± 0.06 mm yr^{-1} ($P < 0.05$; Figures 2B & S7-S8). This compounding effect of the increased wet-season P–ET and decreased dry-season P–ET caused a significant increasing trend in the AR on a hemispheric scale. Spatially, more than half (56.1%) of the land areas showed increasing trends in the wet season P–ET. Among these areas, 6.8% of the land areas significantly increased ($P < 0.05$). For the dry season P–ET, 61.7% (9.6% significantly different ($P < 0.05$)) of the land areas showed decreasing trends and 38.3% (2.1% significantly different ($P < 0.05$)) of the land areas showed increasing trends (Figures 2C–D & S5-S7).

Causes of the trends in land water availability

Since P minus ET was used to represent the land water availability, the changing pattern in the AR can be attributed to the changes in P and ET.[32,33] We applied a simple attribution approach to quantify how the changes in the P and ET shape the observed AR trends. Figure 3 shows the separate contributions of P (Figure 3A) and ET (Figure 3B) to the changes in the AR and their corresponding latitude patterns (Figures 3C-D). The positive and negative contributions of P to the AR trends were widespread, and the positive contributions of ET to the AR trends were concentrated in the high latitude (boreal) region (> 50° N). These different contribution patterns were also evident in their latitude patterns. In the temperate region (23.5–50° N), changes in P played a major role in driving the AR, while in the boreal region, changes in ET mainly caused the AR trends (Figure 3E). Moreover, these two regions exhibited different increasing rates in the AR at 0.34 mm yr^{-1} and 0.21 mm yr^{-1} in the temperate and boreal regions (Figure 3F)., respectively. This phenomenon demonstrated the important role of changes in P in driving an increased AR during the study period.

The contributions of the changes in P and ET to the wet and dry season P–ET were also examined (Figures S9-S10). For the wet season P–ET, in the temperate regions, the changes in P had a positive contribution but the changes in ET played a negative role. In most of the boreal regions, the changes in P and ET contributed positively, indicating that the increased wet season P–ET was mostly driven by changes in P (Figure S9). For the dry season P–ET, changes in P played a positive role in most of the regions in the Northern Hemisphere, while the changes in ET played a negative role in all the regions (Figure S10). In summary, the increased wet season P–ET was primarily driven by changes in P, while the decreased dry season P–ET was mostly driven by the changes in ET. Additionally, in the temperate regions, the increased AR may have been due to the increased wet season P–ET, which was driven by P; in the boreal regions, the increased AR may have been due to the decreased dry season P–ET, which was driven by ET (Figure 3E).

Performance of the CMIP6 models

Based on the observed spatiotemporal AR trends, we also detected whether CMIP6 ESMs capture these observed changes at the hemispheric scale, though most of them can reproduce at the global scale.[12] Using outputs from 32 coupled ESMs (Table S1), we computed AR trends over 2000–2014 for each model and for the multi-model ensemble (Figure 4). We found that 22 of the 32 models successfully reproduced the observed seasonal P–ET trends, whereas 10 models failed to do so (Figure 4). This indicates that the majority of current ESMs can reasonably simulate the seasonality of P–ET, although some models still struggle in certain regions. Moreover, the AR trend ensemble mean of all 32 models (0.07 mm yr^{-1}) closely matched the observed average seasonal P–ET trend (0.09 mm yr^{-1}) (Figure S11), suggesting that while individual models may differ, the ensemble provides a relatively reliable representation of large-scale seasonal patterns. These results imply that, although most models capture the broad seasonal patterns, caution is still warranted when relying solely on individual ESMs to depict or project seasonal P–ET.[1,15,17,20,21,32,40,41]

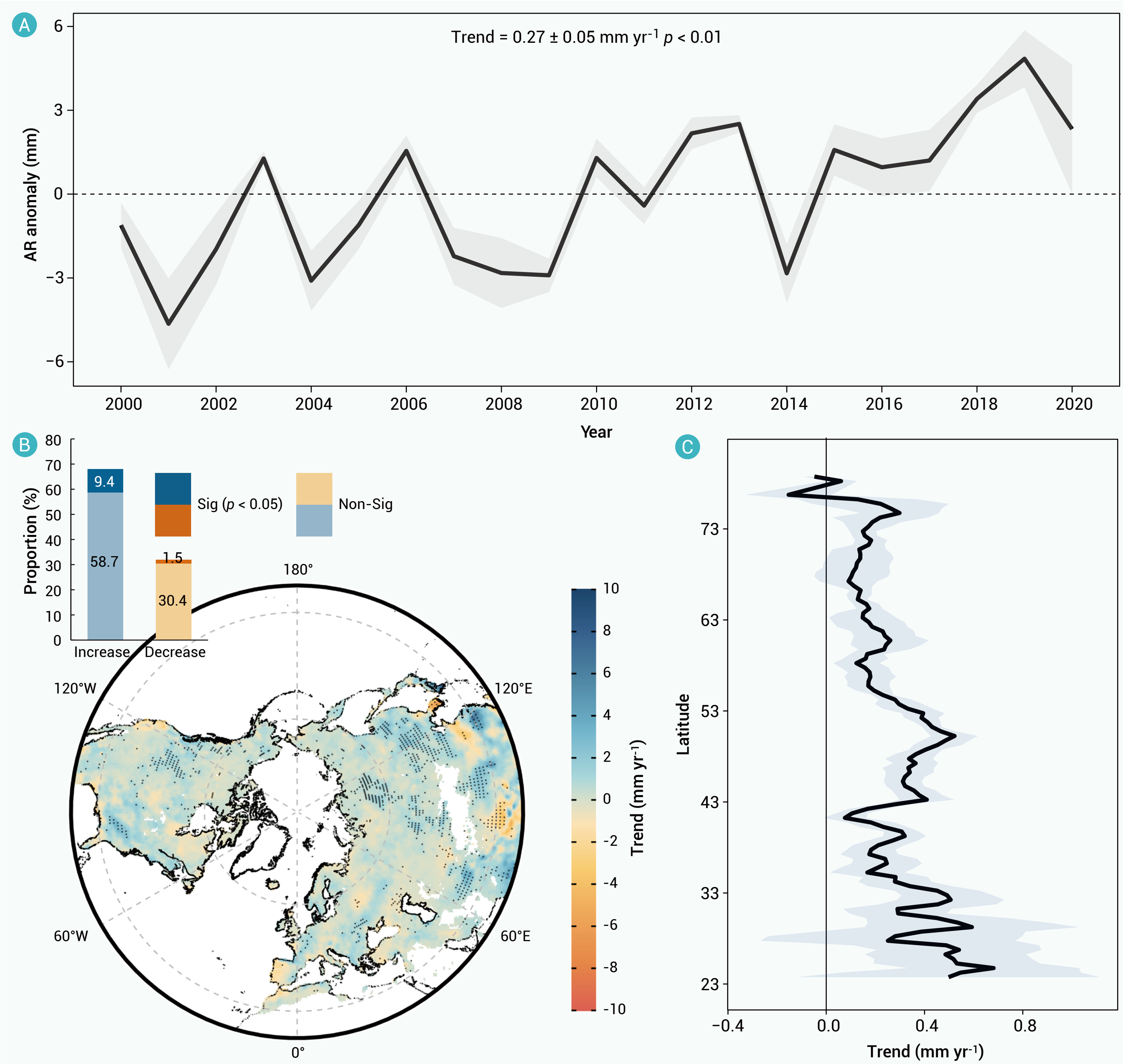

Figure 1. Spatial and temporal changing trends of the annual range (AR) between the wet and dry season water availability in the Northern Hemisphere (A) Time series of the AR from 2000 to 2020. The solid line and shading denote the mean and one standard deviation (SD) of the nine estimates, respectively. (B) Spatial trend in the AR at each 0.5° by 0.5° grid cell across the Northern Hemisphere. The stippling denotes statistically significant trends at $P < 0.05$. The histogram indicates the distribution of the trend in the AR. Abbreviations: sig, significant trends at $P < 0.05$; non-sig, non-significant ($P > 0.05$) change. (C) Aggregated trend in the AR along latitude (mm yr^{-1}). The solid line and shading denote the mean and one SD of the nine estimates, respectively.

DISCUSSION

Changes in P–ET seasonality

Integrated remote sensing and ground-based data show a pronounced widening in the contrast of water availability between wet and dry seasons, indicating a substantial intensification of the water cycle over the past two decades. This growing seasonal disparity raises concern for water resources planning and risk management, particularly across the Northern Hemisphere where water availability directly affects ecosystems, food production, and socio-economic systems. Our results therefore suggest that assessments of water availability should move beyond changes in annual means and explicitly account for shifts in seasonal distribution in the Northern Hemisphere. This phenomenon observed from 2000 to 2020 may continue in the future.[1,17,20] For example, studies based on CMIP6 and CMIP5 ESMs confirmed an increased pattern in the AR in the extratropical Northern Hemisphere and demonstrated a diminishing seasonality of water availability across subtropical regions by comparing historical observations and future projections.[1] This increase in the AR was also projected to increase further as a warmer atmosphere holds more moisture, enhancing large-scale vapor transport and then amplifying the seasonal cycle of water availability.[15] In our evaluation of 32 CMIP6 models, 22 models successfully captured the observed seasonal P–ET trends, and the ensemble mean closely matched the observed average, demonstrating that most current models can reasonably simulate large-scale seasonal patterns. However, 10 models failed to reproduce the observed

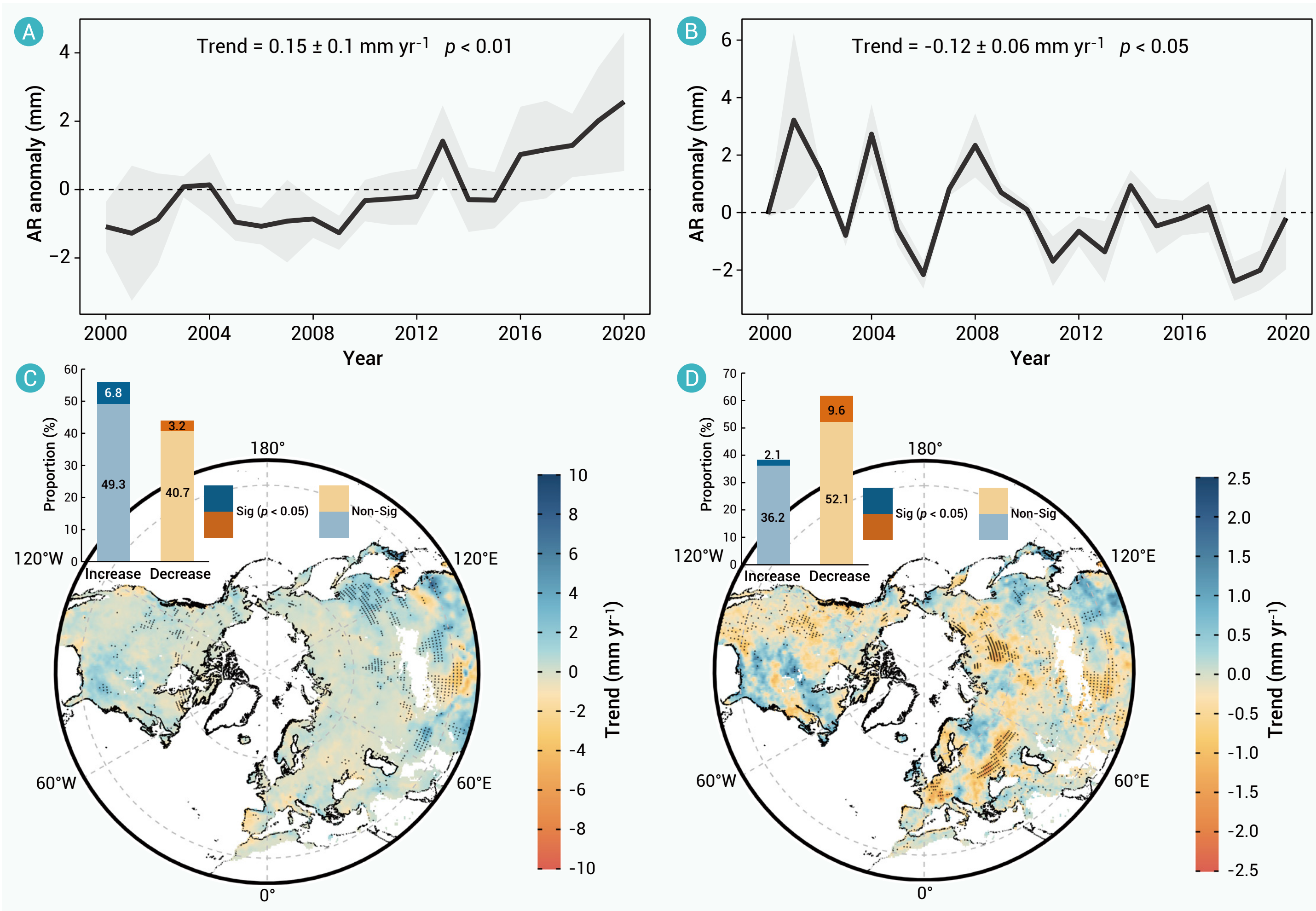

Figure 2. Spatial and temporal changing trends of the wet and dry season water availability (WA) in the Northern Hemisphere (A), (B) Time series of the wet season and dry season WA from 2000 to 2020. The solid line and shading denote the mean and one standard deviation of the nine estimates, respectively. (C), (D)Spatial trend in the wet season and dry season WA at each 0.5° by 0.5° grid cell across the Northern Hemisphere. The stippling denotes statistically significant trends at $P < 0.05$. The histogram indicates the distribution of the trends in the wet and dry season WA. Abbreviations: sig, significant trends at $P < 0.05$; non-sig, non-significant ($P > 0.05$) change.

trends in certain regions, likely due to differences in methodological assumptions and process representations. Our study defines seasonal water availability using P–ET, which primarily captures surface water fluxes, whereas ensemble models often incorporate additional hydrological components such as soil moisture, groundwater, and snowmelt. These differences can influence the estimated seasonality of water availability. Additionally, biases in model parameterizations, particularly regarding vegetation responses, land-atmosphere interactions, and precipitation dynamics, may contribute to the observed inconsistencies.[40]

To examine whether the changes in P–ET are related to climate warming, we tested the relationship between P–ET and temperature changes from 2000 to 2020 and compared with an idealized modeling analysis of Clausius-Clapeyron (CC) relation under climate warming.[42] Specifically, we compared the observed and simulated changes in P–ET seasonality with the expected ~7%/°C scaling of atmospheric moisture content. We found that the seasonal disparity of P-E increases at an average rate of 6.06%/°C (Figure S12), only slightly smaller than the ~7%/°C in CC relation but higher than that of the global trend.[12,42] Our results thus indicate that rising temperatures are accompanied by an amplification of P–E seasonality at the hemispheric scale.[43,44] Further analyses using a simple attribution method revealed the dominant role of P and ET in increasing the wet season P–ET and decreasing the dry season P–ET, respectively. These findings are also supported by previous reports that highlighted the increased rate of P in the wet season as a cause for the increase in water availability.[15] Our results also highlighted the dominant role ET played in the decreased dry season water availability, which is consistent with our global findings.[12] This pattern aligns with the notion that rising atmospheric moisture demand is becoming more spatially widespread and less confined to particular seasons.[32] Within the extratropical Northern Hemisphere, we identify a regime contrast in which changes in wet-dry season P–ET are predominantly precipitation-driven across many temperate regions, whereas evapotranspiration becomes the dominant regulator across large parts of the boreal zone. By resolving where and why P or ET governs the seasonal range, the extratropical Northern Hemisphere analysis provides diagnostics for interpreting regional drought/flood risk and offers more actionable constraints for evaluating and improving Earth system models than a global assessment alone. The significant decline in the dry season water availability is likely to reverberate beyond hydrology, because vegetation growth and productivity respond strongly to water limitation.[45-47] For example, vegetation productivity is more sensitive to dry season water availability,[6] this trend may weaken the land carbon sink. It is also essential to implement measures to mitigate and adapt to seasonal variations of water availability consider its continuous decline under ongoing warming.[32] Underlying drivers of P and ET changes is key to understand the seasonal variations of water availability, though this is beyond the scope of this study. Precipitation patterns are strongly influenced by large-scale atmospheric circulation shifts.[2] For example, alterations in storm track locations, variations in moisture transport from oceanic and terrestrial sources, and changes in cyclone frequency and intensity all play critical roles in modulating seasonal precipitation trends. These dynamic processes determine not only the amount of precipitation but also its temporal distribution, directly affecting seasonal water availability.[15,48] Similarly, seasonal trends in ET are governed by multiple climatic and biophysical factors, such as the rising temperatures and land-use changes (e.g., afforestation).[49] Future studies can incorporate diagnostic analyses of atmospheric circulation indices (e.g., AO,

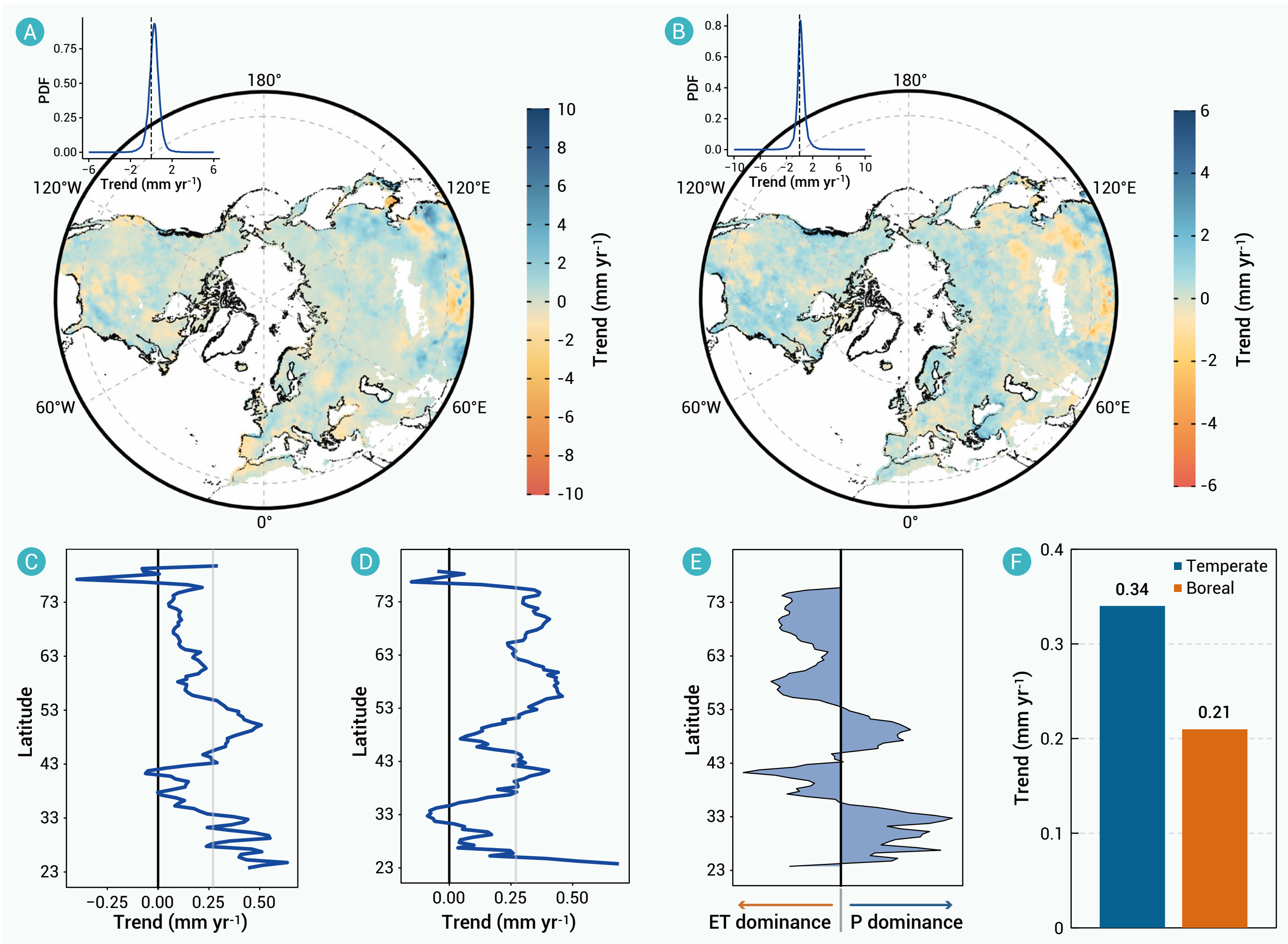

Figure 3. Relative contributions of precipitation and evapotranspiration (P) changes (ET) to shifts in the annual range (AR) (A) Contribution of the changes in P to the AR change. (B) Contribution of the changes in ET to the AR change. The density plots indicate the distribution of the contributions of P and ET to the AR. (C), (D) Latitude patterns of the P and ET contributions to the AR. The grey vertical lines indicate the annual trend of the AR (depicted in Figure 1A). (E) Latitude pattern of the dominant factors (P and ET) affecting the changes in the AR. (F) Trend of the AR in the temperate (23.5°–50° N) and boreal regions (> 50° N).

ENSO, and monsoon indices) and utilize land surface models to quantify the relative contributions of temperature, radiation, and land-use changes to ET trends. By considering these broader climatic and terrestrial drivers, we can refine our understanding of how P–ET seasonality responds to ongoing climate and land-use changes.

Implications

The increase in the AR has several implications for water resources management and ecological restoration.[37,50] Effective measures are required to improve water allocation during the dry season, ensuring that both ecosystem functioning and agricultural production can be sustained. In contrast, wet season management should focus on anticipating and reducing waterlogging risks through proactive drainage and land-use planning. This may involve enhancing the storage and conservation systems of water resources and the implementation of policies for efficient water resource management.[5,51,52] It is also vital to consider seasonal differences in water availability to ensure the sustainability of vegetation growth and ecosystems. For example, the measures regarding vegetation restoration should be adjusted based on seasonal variations in water resources to ensure adequate water for the vegetation throughout the entire year.[49] In addition, the increasing seasonality of water availability observed in the Northern Hemisphere suggests potential global implications, particularly for regions with similar hydroclimatic conditions. As climate change intensifies precipitation extremes and alters evapotranspiration dynamics, other mid-latitude and high-altitude regions may experience widening seasonal water gaps, exacerbating flood and drought risks.

Limitations

The definition of wet and dry seasons in this study is based on the annual maxima and minima of three-month averaged P–ET. While this approach effectively captures precipitation and evapotranspiration dynamics in many regions, it may introduce uncertainties in areas where snowmelt and subsurface water storage play dominant roles in seasonal water availability. In snow-affected regions of the Northern Hemisphere, precipitation often accumulates as snow during winter and does not immediately contribute to surface water availability. Instead, the delayed release of water through snowmelt in spring and early summer constitutes a critical component of seasonal hydrological cycles.[53] Similarly, in regions where soil moisture and groundwater exert substantial control over dry-season water availability, relying solely on P–ET may not capture the full spectrum of hydrological processes. Soil moisture and groundwater serve as crucial buffers, sustaining evapotranspiration and streamflow during low-precipitation periods.[54,55] The omission of these subsurface contributions could result in uncertainties, particularly in arid and semi-arid regions where deep water reserves play a pivotal role in seasonal water supply. Future studies should incorporate snowmelt-driven hydrological processes and subsurface water storage dynamics. This could involve integrating snow water equivalent data, modeled snowmelt fluxes, or groundwater recharge estimates into the analysis. Additionally, comparisons

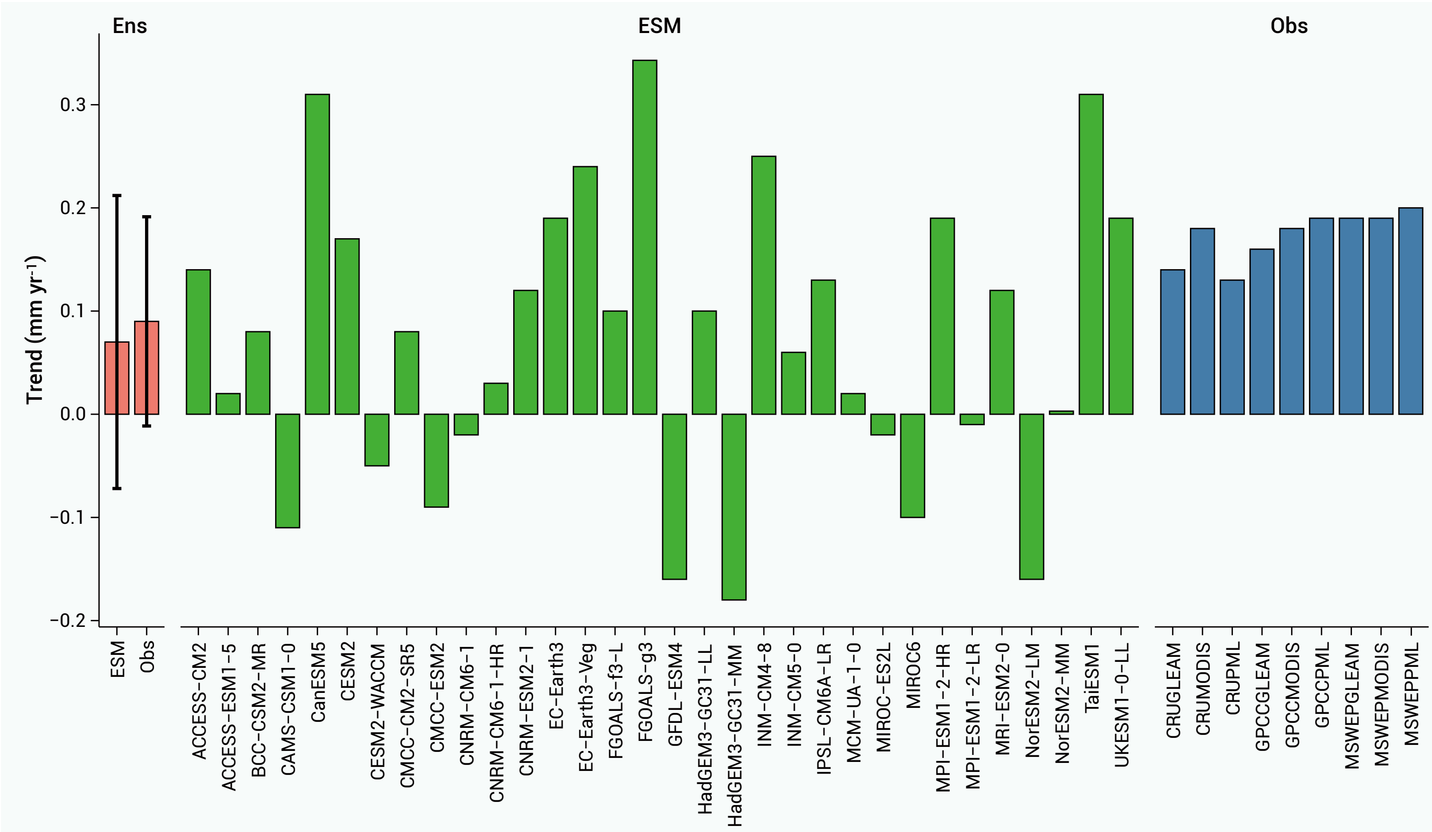

Figure 4. Observed versus modelled trends in AR (wet–dry season water availability) for 2000–2014 Orange bars denote ensemble means across 32 CMIP6 ESMs and nine observational estimates; green and blue bars show individual model and observational estimates, respectively. Black whiskers indicate ±1 standard deviation. Ens, ensemble mean; ESM, Earth system model; Obs, observation-based estimate.

with observed streamflow, soil moisture reanalysis datasets, and GRACE-based terrestrial water storage anomalies could help validate and refine the P–ET-based seasonal definitions.[56] In addition, seasonal changes in P–ET could also be assessed by explicitly defining wet and dry seasons, which may reveal shifts in their onset and duration. However, the timing of wet/dry seasons varies markedly across hydro-climatic regions, posing challenges for a consistent large-scale definition. While beyond the scope of this study, such an approach represents a valuable direction for future work to further elucidate the temporal dynamics of water availability under climate warming.

CONCLUSION

In conclusion, a significantly increasing range was found between wet and dry season water availability during recent decades. This increase in the AR could result in more extreme conditions (more floods or droughts), with potentially impacts on the local hydrology. This increase in the AR is attributed to the compounding effects of increased wet season P–ET and decreased dry season P–ET. The increased wet season P–ET was mostly driven by the changes in P, while changes in ET were the main cause of the decreased dry season P–ET. Evaluation of 32 state-of-the-art ESMs shows that most models (22 of 32) capture these seasonal trends, and the ensemble mean closely matches observations, although some models fail in certain regions. These results highlight both the reliability of current models for large-scale seasonal patterns and the need for caution in using individual models for regional assessments. The findings of this study would be valuable to formulate appropriate policies regarding water resources management in the context of climate change.

REFERENCES

1. Zhou S., Williams A. P., Lintner B. R., et al. (2022). Diminishing seasonality of subtropical water availability in a warmer world dominated by soil moisture-atmosphere feedbacks. *Nat. Commun.* 13:5756. DOI:10.1038/s41467-022-33473-9
2. Zhang Y., Li C., Chiew F. H. S., et al. (2023). Southern Hemisphere dominates recent decline in global water availability. *Science* 382:579–584. DOI:10.1126/science.adh0716
3. Seddon A. W., Macias-Fauria M., Long P. R., et al. (2016). Sensitivity of global terrestrial ecosystems to climate variability. *Nature* 531:229–232. DOI:10.1038/nature16986
4. Kotz M., Levermann A. and Wenz L. (2022). The effect of rainfall changes on economic production. *Nature* 601:223–227. DOI:10.1038/s41586-021-04283-8
5. Huggins X., Gleeson T., Kummu M., et al. (2022). Hotspots for social and ecological impacts from freshwater stress and storage loss. *Nat. Commun.* 13:439. DOI:10.1038/s41467-022-28029-w
6. Murray-Tortarolo, G., P. Friedlingstein, S. Sitch, S. I. et al. (2016). The dry season intensity as a key driver of NPP trends. *Geophys. Res. Lett.* 43:2632–2639. DOI:10.1002/2016GL068240
7. Jung M., Reichstein M., Ciais P., et al. (2010). Recent decline in the global land evapotranspiration trend due to limited moisture supply. *Nature* 467:951–954. DOI:10.1038/nature09396
8. Allan R. P., Barlow M., Byrne M. P., et al. (2020). Advances in understanding large-scale responses of the water cycle to climate change. *Ann. N. Y. Acad. Sci.* 1472:49–75. DOI:10.1111/nyas.14337
9. Held I. M. and Soden B. J. (2006). Robust responses of the hydrological cycle to global warming. *J. Clim.* 19:5686–5699. DOI:10.1175/jcli3990.1
10. Allan R. P. (2023). Amplified seasonal range in precipitation minus evaporation. *Environ. Res. Lett.* 18:094004. DOI:10.1088/1748-9326/acea36
11. Intergovernmental Panel on Climate C. (2023). Climate change 2021 – The physical science basis: Working hroup I contribution to the sixth assessment report of the intergovernmental panel on climate change (Cambridge University Press). DOI:10.1017/9781009157896
12. Shi W., Zhao F., Wang Q., et al. (2026). Amplified global seasonality in water availability over land in recent decades. *J. Clim.* 39:249-259. DOI:10.1175/JCLI-D-24-0768.1
13. Kumar S., Allan R. P., Zwiers F., et al. (2015). Revisiting trends in wetness and dryness in the presence of internal climate variability and water limitations over land. *Geophys. Res. Lett.* 42:867-875. DOI:10.1002/2015gl066858
14. Chou C., Neelin J. D., Chen C.-A., et al. (2009). Evaluating the "rich-get-richer" mechanism in tropical precipitation change under global earming. *J. Clim.* 22:1982-2005. DOI:https://doi.org/10.1175/2008JCLI2471.1
15. Chou C. and Lan C.-W. (2012). Changes in the annual range of precipitation under global warming. *J. Clim.* 25:222–235. DOI:10.1175/jcli-d-11-00097.1
16. Liu C. and Allan R. P. (2013). Observed and simulated precipitation responses in wet and dry regions 1850–2100. *Environ. Res. Lett.* 8:034002. DOI:10.1088/1748-9326/8/

3/034002
17. Chou C., Chiang J. C. H., Lan C.-W., et al. (2013). Increase in the range between wet and dry season precipitation. *Nat. Geosci.* 6:263–267. DOI:10.1038/ngeo1744
18. Zaitchik B. F., Rodell M., Biasutti M., et al. (2023). Wetting and drying trends under climate change. *Nat. Water* 1:502–513. DOI:10.1038/s44221-023-00073-w
19. Greve P., Orlowsky B., Mueller B., et al. (2014). Global assessment of trends in wetting and drying over land. *Nat. Geosci.* 7:716–721. DOI:10.1038/ngeo2247
20. Byrne M. P. and O'Gorman P. A. (2015). The response of precipitation minus evapotranspiration to climate warming: Why the "wet-get-wetter, dry-get-drier" scaling does not hold over land. *J. Clim.* 28:8078-8092. DOI:10.1175/JCLI-D-15-0369.1
21. Mankin J. S., Seager R., Smerdon J. E., et al. (2019). Mid-latitude freshwater availability reduced by projected vegetation responses to climate change. *Nat. Geosci.* 12:983–988. DOI:10.1038/s41561-019-0480-x
22. Kumar S., Lawrence D. M., Dirmeyer P. A., et al. (2014). Less reliable water availability in the 21st century climate projections. *Earth's Future* 2:152-160. DOI:https://doi.org/10.1002/2013EF000159.
23. Zhao F., Wang X., Wu Y., et al. (2023). Prefectures vulnerable to water scarcity are not evenly distributed across China. *Commun. Earth Environ.* 4:145. DOI:10.1038/s43247-023-00808-3
24. Piao S., Ciais P., Huang Y., et al. (2010). The impacts of climate change on water resources and agriculture in China. *Nature* 467:43–51. DOI:10.1038/nature09364
25. Jiao W., Wang L., Smith W. K., et al. (2021). Observed increasing water constraint on vegetation growth over the last three decades. *Nat. Commun.* 12:3777. DOI:10.1038/s41467-021-24016-9
26. Harris I., Osborn T. J., Jones P., et al. (2020). Version 4 of the CRU TS monthly high-resolution gridded multivariate climate dataset. *Sci. Data* 7:109. DOI:10.1038/s41597-020-0453-3
27. Schneider D. P., Deser C., Fasullo J., et al. (2013). Climate data guide spurs discovery and understanding. *Trans. Amer. Geophys. Union* 94:121-122. DOI:10.1002/2013EO130001
28. Beck H. E., Wood E. F., Pan M., et al. (2019). MSWEP V2 global 3-hourly 0.1° precipitation: Methodology and quantitative assessment. *Bull. Am. Meteorol. Soc.* 100:473-500. DOI:10.1175/BAMS-D-17-0138.1
29. Martens B., Miralles D. G., Lievens H., et al. (2016). GLEAM v3: Satellite-based land evaporation and root-zone soil moisture. *Geosci. Model Dev. Discuss.* DOI:10.5194/gmd-2016-162
30. Mu Q., Zhao M. and Running S. W. (2011). Improvements to a MODIS global terrestrial evapotranspiration algorithm. *Remote Sens. Environ.* 115:1781-1800. DOI:10.1016/j.rse.2011.02.019
31. Zhang Y., Kong D., Gan R., et al. (2019). Coupled estimation of 500 m and 8-day resolution global evapotranspiration and gross primary production in 2002–2017. *Remote Sens. Environ.* 222:165–182. DOI:10.1016/j.rse.2018.12.031
32. Padrón R. S., Gudmundsson L., Decharme B., et al. (2020). Observed changes in dry-season water availability attributed to human-induced climate change. *Nat. Geosci.* 13:477–481. DOI:10.1038/s41561-020-0594-1
33. Zhao F., Ma S. and Wu Y. (2021). Changes in dry-season water availability and attributions in the Yellow river basin, China. *Front. Environ. Sci.* 9:762137. DOI:10.3389/fenvs.2021.762137
34. Theil H. (1992). Henri Theil's contributions to economics and econometrics: econometric theory and methodology. Baldev Raj, Johan Koerts (eds). Springer Science & Business Media. DOI:10.1007/978-94-011-2546-8
35. Sen P. K. (1968). Estimates of the regression coefficient based on Kendall's tau. *J. Am. Stat. Assoc.* 63:1379–1389. DOI:10.1080/01621459.1968.10480934
36. Mann H. B. (1945). Nonparametric tests against trend. Econometrica, pp:245-259. DOI:10.2307/1907187
37. Kendall M. G. (1948). Rank correlation methods. https://publ.lib.ru/ARCHIVES/Z/''Zarubejnye_statisticheskie_issledovaniya''_(seriya)/%CA%E5%ED%E4%FD%EB%20%CC._%20%D0%E0%ED%E3%EE%E2%FB%E5%20%EA%EE%F0%F0%E5%EB%FF%F6%E8%E8.(1975).pdf
38. Gillett N. P., Shiogama H., Funke B., et al. (2016). The detection and attribution model intercomparison project (DAMIP v1. 0) contribution to CMIP6. *Geosci. Model Dev.* 9:3685-3697. DOI:10.5194/gmd-9-3685-2016
39. Eyring V., Bony S., Meehl G. A., et al. (2016). Overview of the coupled model intercomparison project phase 6 (CMIP6) experimental design and organization. *Geosci. Model Dev.* 9:1937–1958. DOI:10.5194/gmd-9-1937-2016
40. Zhao F., Wu Y., Yin X., et al. (2022). Projected changes in population exposure to drought in China under CMIP6 forcing scenarios. *Atmos. Environ.* 282:119162. DOI:10.1016/j.atmosenv.2022.119162
41. Greve P. and Seneviratne S. I. (2015). Assessment of future changes in water availability and aridity. *Geophys. Res. Lett.* 42:5493-5499. DOI:10.1002/2015GL064127
42. Alduchov O. A. and Eskridge R. E. (1996). Improved Magnus form approximation of saturation vapor pressure. *J. Appl. Meteorol.* 35:601-609. DOI:10.1175/1520-0450(1996)035%3C0601:IMFAOS%3E2.0.CO;2
43. Ghausi S. A. and Ghosh S. (2020). Diametrically opposite scaling of extreme precipitation and streamflow to temperature in South and Central Asia. *Geophys. Res. Lett.* 47. DOI:10.1029/2020gl089386
44. Ivancic T. J. and Shaw S. B. (2016). AU.S. - based analysis of the ability of the Clausius - Clapeyron relationship to explain changes in extreme rainfall with changing temperature. *J. Geophys. Res. Atmos.* 121:3066–3078. DOI:10.1002/2015jd024288
45. Li W., Migliavacca M., Forkel M., et al. (2022). Widespread increasing vegetation sensitivity to soil moisture. *Nat. Commun.* 13:3959. DOI:10.1038/s41467-022-31667-9
46. Liu L., Ciais P., Wu M., et al. (2023). Increasingly negative tropical water-interannual CO_2 growth rate coupling. *Nature* 618:755–760. DOI:10.1038/s41586-023-06056-x
47. Humphrey V., Zscheischler J., Ciais P., et al. (2018). Sensitivity of atmospheric CO_2 growth rate to observed changes in terrestrial water storage. *Nature* 560:628–631. DOI:10.1038/s41586-018-0424-4
48. Konapala G., Mishra A. K., Wada Y., et al. (2020). Climate change will affect global water availability through compounding changes in seasonal precipitation and evaporation. *Nat. Commun.* 11:3044. DOI:10.1038/s41467-020-16757-w
49. Zhao F., Ma S., Wu Y., et al. (2022). The role of climate change and vegetation greening on evapotranspiration variation in the Yellow River Basin, China. *Agr. Forest Meteorol.* 316:108842. DOI:10.1016/j.agrformet.2022.108842
50. Zhao F., Wu Y., Yin X., et al. (2022). Toward sustainable revegetation in the Loess Plateau using coupled water and carbon management. *Eng.* 15:143–153. DOI:10.1016/j.eng.2020.12.017
51. Zhou F., Bo Y., Ciais P., et al. (2020). Deceleration of China's human water use and its key drivers. *Proc. Natl. Acad. Sci. USA* 117:7702–7711. DOI:10.1073/pnas.1909902117
52. Fu, J., Jian, Y., Wang, X. et al. (2023). Extreme rainfall reduces one-twelfth of China's rice yield over the last two decades. *Nat. Food* 4. DOI:10.1038/s43016-023-00753-6.
53. Han J., Liu Z., Woods R., et al. (2024). Streamflow seasonality in a snow-dwindling world. *Nature* 629:1075–1081. DOI:10.1038/s41586-024-07299-y
54. Yao Y., Zheng C., Andrews C. B., et al. (2021). Role of groundwater in sustaining northern himalayan rivers. *Geophys. Res. Lett.*48: e2020GL092354. DOI:10.1029/2020gl092354
55. Rodell M., Famiglietti J. S., Wiese D. N., et al. (2018). Emerging trends in global freshwater availability. *Nature* 557:651–659. DOI:10.1038/s41586-018-0123-1
56. Zan B., Ge J., Mu M., et al. (2024). Spatiotemporal inequality in land water availability amplified by global tree restoration. *Nat. Water* 2:863–874. DOI:10.1038/s44221-024-00296-5

FUNDING AND ACKNOWLEDGMENTS

This work was supported by the National Natural Science Foundation of China (U25A20758 and 42271025); the Innovation Team of Shaanxi Province (2021TD-52); the Technology Innovation Center for Land Engineering and Human Settlements, Shaanxi Land Engineering Construction Group Co. Ltd. and Xi'an Jiaotong University (201912131B2); the National Natural Science Foundation of China (42101029); and the China Postdoctoral Science Foundation (2020M683451 and 2022T150513). The funders had no role in study design, data collection and analysis, decision to publish, or preparation of the manuscript.

AUTHOR CONTRIBUTIONS

F.B.Z. conceived the idea and designed the research. W.B.S. carried out the data analysis. F.B.Z., Y.P.W., and S.G.L prepared the original draft. All authors contributed to the manuscript and approved the final version.

DECLARATION OF INTERESTS

The authors declare no competing interests.

DATA AND CODE AVAILABILITY

The CRU precipitation data were obtained from https://crudata.uea.ac.uk/cru/data/hrg/, the GPCC data is available at https://psl.noaa.gov/data/gridded/data.gpcc.html, and the MSWEP data is available at https://www.gloh2o.org/mswep/. The GLEAM ET data were obtained from https://www.gleam.eu/ and the PML-V2 data are available at https://data.tpdc.ac.cn/zh-hans/data/48c16a8d-d307-4973-abab-972e9449627c/. CMIP6 model simulations are available from https://esgf-node.llnl.gov/search/cmip6/. Data and code are available from the corresponding author upon reasonable request.

SUPPLEMENTAL INFORMATION

It can be found online at https://doi.org/10.59717/j.xinn-geo.2026.100191